

Size and Shape Effects on Fracture Strength of Concrete

Hau-Kit Man¹ & Jan G.M. van Mier²

Materials Research Center, Institute for Building Materials

Department of Civil, Environmental and Geomatic Engineering (D-BAUG)

ETH Zurich

Schafmattstr. 6, 8093 Zürich, Switzerland

¹hkman@ethz.ch, ²jvanmier@ethz.ch

ABSTRACT: Three-dimensional size and shape effects on concrete fracture are studied by means of a series of simulations of the fracture behaviour of prisms loaded in three-point bending. The simulations have been carried out with a simple beam-lattice model. The meso-structure of concrete is directly included in the model as a three-phase representation comprising aggregate, matrix and the interface between these two phases. Size effects are studied by varying the prism size in either two (constant thickness) or in three-dimensions. Prisms both with and without embedded particle structure were studied (particle densities $P_k = 0\%$ and $P_k = 35\%$). Next to that a series of analyses was performed where the shape of the specimen was varied while maintaining the volume of the structure constant. The analyses show that size and shape effects are conveniently described by means of a power law between strength and specimen volume.

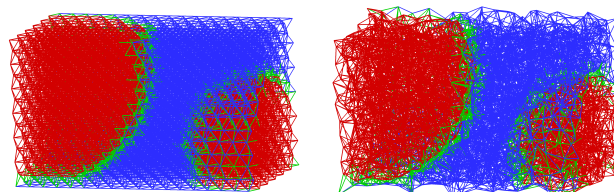
1 INTRODUCTION

This paper investigates the size and shape effect of fracture in three-dimensional concrete structures. In the past, size effect studies are investigated mainly through the simpler two-dimensional scaling (scaling in height and length). Full scaling (in three dimensions) with three-dimensional models is from its concept and implementation very difficult and demanding; because of its complexity it is not common neither in performing laboratory experiments nor in numerical simulations. The fracture experiments, which are described here, were conducted computationally.

As numerical tool a beam lattice model was used. A truss lattice was first introduced in the 1940s for solving problems in elasticity (Hrennikoff 1941); in the 1990s statistical physicists simulated brittle fracture with a beam lattice model (Herrmann et al. 1989). Following this, a modified version of this model was used to simulate fracture experiments for concrete (Schlangen and van Mier 1992), (Schlangen 1993). Alterations were made to ensure realistic mechanical and material properties for concrete. These kinds of simulations can be done either with a regular configuration (i.e. all lattice elements have the same length, see also Figure 1(a)) or with using a random lattice (i.e. lattice elements have different element lengths,

see Figure 1(b)); see (Lilliu and van Mier 2003) and (Man and van Mier 2007).

One major disadvantage in running lattice simulations is the huge computational effort. Because of that, in the beginning these kind of simulations were rather simplified (with small numbers of elements). The models were limited in two dimensions and the implementation of the microstructure lacked in detail. This paper uses an object-oriented version of the lattice program, in which a parallel solver is used suitable for an unlimited number of parallel processors (Lingen 2000). With this improvement and with the



(a) Regular lattice

(b) Random lattice

Figure 1: Material structure of concrete (Cement Matrix: blue, Aggregates: red and the ITZ: green) after overlay of the microstructure in a regular (Figure 1(a)) and a random 3D (Figure 1(b)) lattice.

ongoing development of faster computing systems, it is now possible to include much more detail into the microstructure. Moreover 3D analyses can be carried out within reasonable time span; see (Lilliu and van Mier 2003), (Man and van Mier 2006) and (Man and van Mier 2007).

Also size effect study with 3D models is now possible: In (Van Vliet 2000) and (Man and van Mier 2006) scaling was in two-dimensions (scaling in length and height only) and in three-dimensions with a single constant particle density P_k , while in (Man and van Mier 2007) the influence of different particle densities on size effects were investigated.

In this paper we focus on size and shape effects on concrete fracture, in particular three-dimensional effects are studied. In the past most studies focused on 2D-size effects, although by keeping the size in one direction constant leads to a shape variation that usually is ignored (plane stress to plane strain transition, see (Van Vliet 2000)).

2 NUMERICAL MODEL

2.1 3D Lattice Model

In the beam lattice model, the material is discretized as a network of Bernoulli beams, which can be arranged in either a regular or a random configuration. The intention of this model is to understand the fracture behavior of concrete in general, in particular softening behaviour and the stable micro-fracture processes leading up to the situation from where softening starts.

Concrete is on the meso-level (scale range between 10^{-3} and 10^{-1} m) a highly heterogeneous material. It can be defined as a three-phase material: aggregates, cement matrix and between them the interfacial transition zone (ITZ). The material structure can be generated with a dedicated computer program and it is then overlaid on top of the lattice (see Figure 1).

Fracture is simulated by a sequential removal of a single element from the mesh in each step. Until failure, lattice elements behave linear elastic. Sequentially the lattice element with the most critical (the highest) stress over tensile strength ratio (σ/f_t), will be removed according to the simple failure law:

$$\frac{\sigma}{f_t} = \frac{1}{f_t} \left(\frac{N}{A} + \alpha \frac{\max(M_i, M_j)}{W} \right) \quad (1)$$

A is the cross-section area and W is the section modulus. N is the normal force and M_i, M_j are the effective bending moments of the nodes i and j . α is a parameter, which defines the role of bending in the fracture. Usually α has a value ranging between 0 and 0.005.

2.2 Overview of Analyses

As mentioned three-dimensional prisms of different sizes subjected to three-point bending are

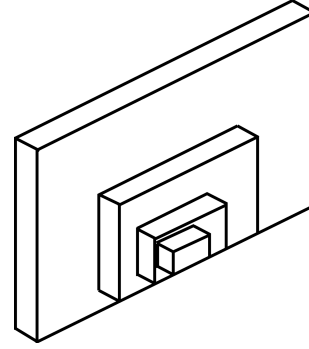


Figure 2: Case study I: 2D Scaling; see Table 1

	Size [mm]	# Elements	Vol. [mm ³]
small	4.375 x 2.5 x 2.5	15073	27.35
medium	8.75 x 5 x 2.5	62533	109.38
large	17.5 x 10 x 2.5	251091	437.5
Xlarge	35 x 20 x 2.5	985133	1750

Table 1: Geometries of the case study I: 2D-scaling; see Figure 2

simulated and analyzed (see Figure 2 to Figure 5). All lattice elements have a circular cross section and the diameter d was set to $d = 0.144$ mm guaranteeing a Possion's ratio $\nu = 0.2$. The ratios for the three material phases are: $E_{agg}/E_{mat}/E_{ITZ} = 70000/25000/25000$ (Young's moduli) and $f_{t,agg}/f_{t,mat}/f_{t,ITZ} = 10/5/1.25$ (tensile strength of the lattice elements). The aggregate diameters range from 0.5 mm to 2 mm and the distribution obeys a Fuller curve.

Different particle densities were used: a particle density with $P_k = 35\%$ in a regular lattice configuration, a purely homogeneous cement matrix ($P_k = 0\%$), both in a regular and a random configuration.

The specimen volumes ranges from 13.67 mm³ (4.375 x 2.5 x 1.25 mm, 7831 elements) to 14000 mm³ (35 x 20 x 20 mm, 7448373 elements). Four different cases are investigated: 2D scaling (Figure 2, Table 1), 3D scaling (Figure 3, Table 2) on prisms with a quadratic profile, 3D scaling on prisms with a rectangular profile (Figure 4, Table 3) and as a special case various prisms with identical volumes, but varying shape (see Figure 5, Table 4).

For the case of using a regular triangular lattice configuration, the element length of 0.25 mm is chosen. For the case of simulating irregular lattices, the element length are randomly distributed between 0.125 mm and 0.375 mm.

	Size [mm]	# Elements	Vol. [mm ³]
small	4.375 x 2.5 x 2.5	15073	27.35
medium	8.75 x 5 x 5	122593	218.75
large	17.5 x 10 x 10	974403	1750
Xlarge	35 x 20 x 20	7448373	14000

Table 2: Geometries of the case study II: 3D-scaling on a quadratic profile; see Figure 3

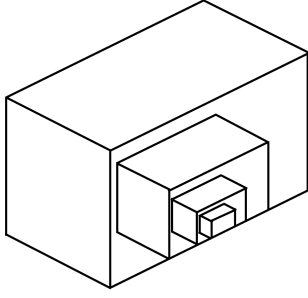


Figure 3: Case study II: 3D Scaling; see [Table 2](#)

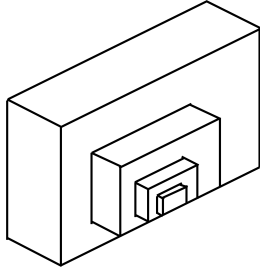


Figure 4: Case study III: 3D Scaling, see [Table 3](#)

Even now, performing lattice simulations with this large number of elements are very time-consuming, the bottleneck is still the lack of computing power. The experiments were performed on two different computer systems: The first system was a Silicon Graphics Altix 350 with 16 Intel Itanium 2 processors with clock-speeds from 1.4 to 1.6 GHz and 32 GB of memory. The second one was the massively parallel processing (MPP) CRAY XT3 computer system with 1656 AMD Opteron (1100 single-core and 556 dual-core) processors from CSCS in Manno (TI), Switzerland.

To determine the most efficient use of processors on the CRAY, various benchmark simulations were performed. [Table 5](#) state one numerical problem running from 1 to 1024 parallel processors with a lattice with 974403 elements ([Table 2](#), specimen 'large'). Column 2 shows the parallel speedup (Amdahl's Law). It is defined as the quotient of the execution time for 1 processor divided by the execution time for the same numerical problem parallelized with n processors; the number simply states how much faster the use of n processors is compared to 1 processor. Column 3 describes the parallel speedup between n compared to n/2 processors. The results point out that the speedup is perfect up to 64 processors, doubling the numbers of processors cuts the computing time nearly in

	Size [mm]	# Elements	Vol. [mm ³]
small	4.375 x 2.5 x 1.25	7831	13.67
medium	8.75 x 5 x 2.5	62533	109.38
large	17.5 x 10 x 5	492195	875
Xlarge	35 x 20 x 10	3665013	7000

Table 3: Geometries of the case study III: 3D-scaling on a rectangular profile; see [Figure 4](#)

	Size [mm]	# Elements	Vol. [mm ³]
A	11.875 x 4.12 x 4.75	124999	233.7
B	10.875 x 5.8 x 3.5	118535	220.76
C	12.375 x 2.815 x 6.5	122243	226.43
D	8.875 x 5 x 5	122593	221.88
E	16 x 3.7 x 3.7	125241	229.04

(a) medium

	Size [mm]	# Elements	Vol. [mm ³]
A	23.75 x 8.25 x 9.5	999988	1861.4
B	21.75 x 11.5 x 7	948280	1750.87
C	25.75 x 5.75 x 12	977924	1776.25
D	17.75 x 10 x 10	974403	1750
E	32 x 7.5 x 7.5	985456	1800

(b) large

Table 4: Geometries of the case study IV; see [Figure 5](#)

half. Compared to the simulation running on 1 processor, the same problem running on 64 processors is around 67 times faster. In this specific case the parallel speedup decreases from 128 processors. The use of larger processors is possible, but usually to simulate one 3D fracture experiment (over 500000 elements) 64 or 128 processors were used.

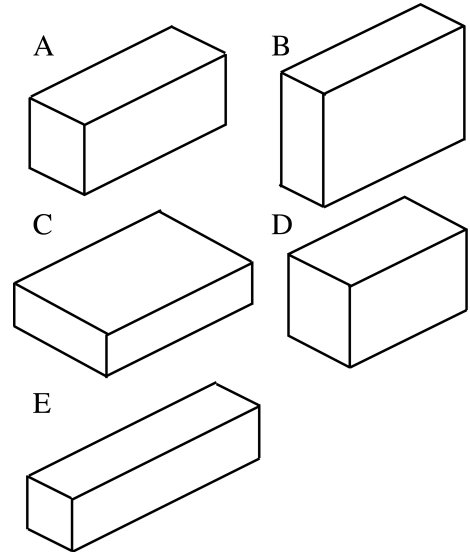


Figure 5: Case study IV; see [Table 4](#).

3 RESULTS

3.1 Size Effect Study

[Figure 6](#) represents for lattice simulations a typical load-displacement diagram for concrete ([Table 2](#), specimen 'medium'). The enveloping curve describes a graph, which is similar to the load-displacement curves found from laboratory experiments. Typical for lattice-type simulations are the zigzags in the diagram after connecting the single steps: this indicates

n	$\frac{T(1)}{T(n)}$	$\frac{T(n/2)}{T(n)}$
1	1	-
2	2.52	2.52
4	4.78	1.89
8	9.41	1.97
16	18.77	1.99
32	35.63	1.90
64	67.06	1.88
128	111.40	1.66
256	190.03	1.71
512	263.24	1.39
1024	300.73	1.14

Table 5: Parallel speedup of the numerical program, n : number of parallel processors used in one simulation, performed on a lattice structure with 974403 elements on the CRAY XT3

the subsequent loading-unloading during element removals. In the diagram, the typical stages of the fracture processes in concrete are found on the diagram (Van Mier 2004): (a)-(b) regime of stable microcracking, (b)-(c) macrocrack growth and (c)-(d) bridging. From these load-displacement diagrams for concrete the maximum forces can be measured and as results the fracture strengths can be calculated according to the theory of linear elasticity. The different strength for the various specimens can be gathered for example in a fracture strengths vs. specimen height diagram (see for example Figure 7 for $P_k = 35\%$). As result the size effect on global specimen strength can be observed. There is a reduction of the nominal strength with larger specimen sizes; similar qualitative observations can be also seen on the laboratory experiments and simulations done by van Vliet (Van Vliet 2000). In terms of $\sigma - H$ relationship, each set of simulations must be described by means of separate bi-logarithmic equations, resulting in different slopes

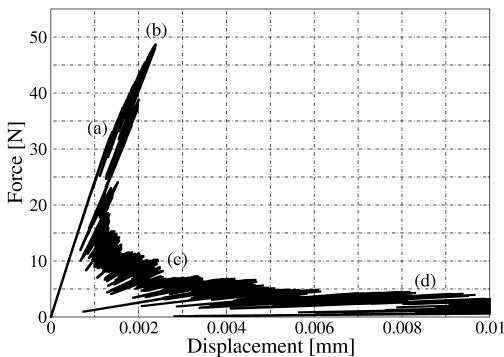


Figure 6: diagram from a 3D concrete prism analyzed with 122593 lattice elements (Table 2, size 'medium') and $P_k = 35\%$. The letters in brackets (a) - (d) show the transition points between the typical stages in the fracture process in concrete

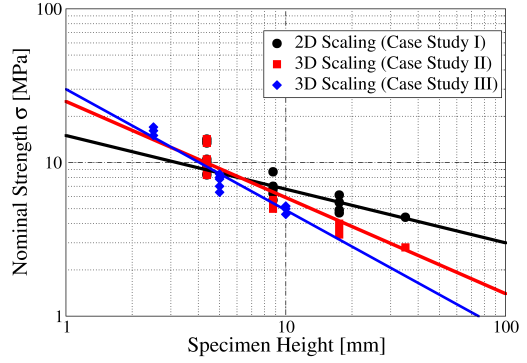


Figure 7: $\log \sigma - \log H$ relationship for $P_k = 35\%$

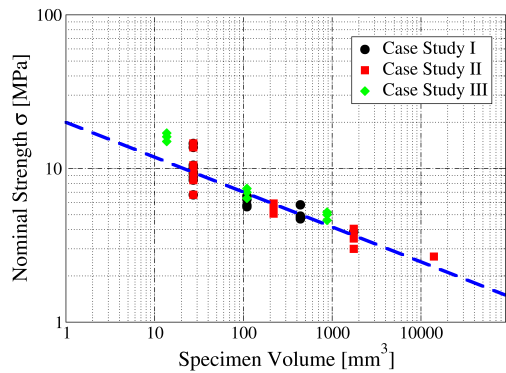


Figure 8: $\log \sigma - \log V$ relationship for $P_k = 35\%$

(see Figure 7). For the case of $P_k = 35\%$ the slope for 2D scaling is 0.5, while for 3D scaling a slope of 0.7 was calculated (Man and van Mier 2006). For the homogenous cement matrix material ($P_k = 0\%$) slopes of 0.22 for 2D scaling and of 0.33 for 3D scaling were obtained for both, regular and random lattices, although the load-displacement curves, the nominal strength and the crack patterns differ significantly between regular and random configurations; for a more extensive discussion, see (Man and van Mier 2007). Instead of a specimen height vs. strength relationship, a specimen volume vs. nominal strength diagram can be constructed ($\log \sigma - \log V$ diagram, see Figure 8 and Figure 9). The main conclusion remains the same: an increasing specimen volume leads to a reduction in strength. However, this diagram shows one additional new observation, which could not be seen in a $\log \sigma - \log H$ -relationship: In that case, all points from the three case studies (2D and 3D scaling cases) fall on a single line (Figure 8 for $P_k = 35\%$, Figure 9 for $P_k = 0\%$ in a regular and random configuration¹).

¹Figure 9 shows one difference between using lattices with regular and random configuration. The strength for regular lattices is significant higher than the random one. The resulting slopes have similar values: therefore the regression lines are parallel.

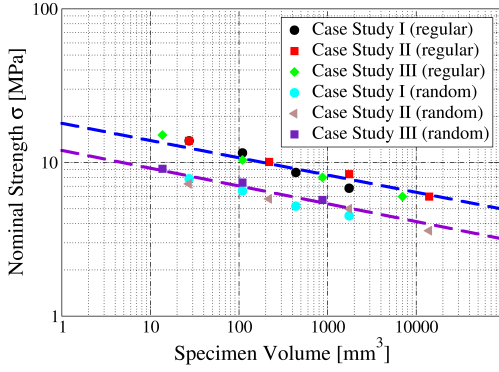


Figure 9: $\log \sigma - \log V$ relationship for $P_k = 0\%$ on a regular and random configuration

In a $\log \sigma - \log V$ relation the behaviour of all structures of varying volume is captured by using a single coefficient, which is more convenient than the separate equations if each case would be considered separately. The question that can be raised now is the following. If not the height, but rather the volume is a more appropriate parameter in a size effect law, could it be that shape effects can be treated similarly? This question will be addressed in the next section.

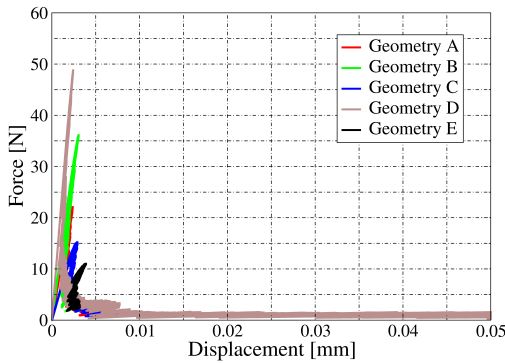


Figure 10: Typical Load-Displacement diagrams for 3D concrete prisms ($P_k = 0\%$, random lattice, 'medium') for case study IV, with the geometries A, B, C and D; see Figure 5

3.2 Shape Effect Study

The fracture strength of a prism loaded in three-point bending can be written as

$$\sigma = \frac{3 Fl}{2 bh^2} \quad (2)$$

It can easily be seen that the fracture strength depends on the length, width and height of the considered prism. We are interested to see what would happen to the $\log \sigma - \log V$ relation when specimen volumes are considered with varying shapes. For that

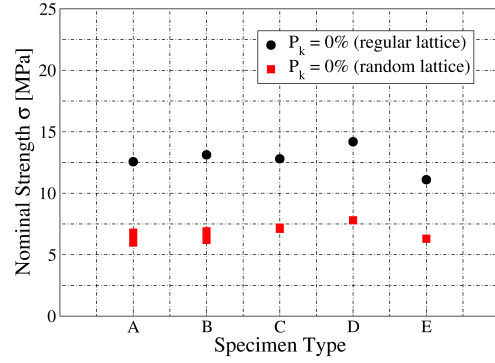


Figure 11: Comparison of the nominal strength for different shapes with identical volumes; case study IV (medium sized specimen)

purpose five different specimens subjected to three-point-bending were analyzed (see Table 4 and Figure 5). The specimens have different proportions (differences in length, height and width), but their volumes are kept constant. Two different sizes are fully scaled (see Table 4), the smaller specimens have 118535 to 125241 lattice elements (see Table 4(a)) while the larger specimens have 948280 to 999988 elements (see Table 4(b)). The fracture experiments will be performed with $P_k = 0\%$ in regular and random configurations.

The load-displacement diagrams (Figure 10, simulated with a random medium-sized lattice) for various geometries show that the maximum loads differ dependent on the specimen shape: the calculated fracture strengths show (Figure 11) that the values are similar (around 6-7 MPa for random and 12-14 MPa for regular lattices²), regardless of the shapes considered here. This may be interesting because the maximum forces and the geometry are different, but the resulting strength remains the same. This fits to the observations made in the previous section (i.e. not contradictory). In this study the material properties and the specimen volume are the only parameters, which are held constant.

Up to this point the strength for the 'medium' specimens are quite close and the same as for the 'large' specimen. For the five different geometries the calculated strength can be included in Figure 9, resulting in the new graph shown in Figure 12. In fact, only two volumes for the different geometries were investigated, the study needs to be extended (specifically the addition of larger sizes), and also for other particle densities P_k .

²Figure 11 also illustrates the difference between simulations done with regular and a random lattices; here: the nominal strength (like in Figure 9)

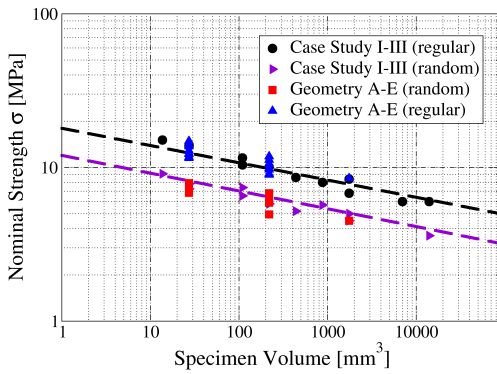


Figure 12: The present calculated nominal strength for the geometries A-E put on the same diagram on [Figure 9](#)

4 SUMMARY AND CONCLUSIONS

In this paper numerical simulations with a 3D beam-lattice model were performed. Specimens subjected to three-point bending were simulated until complete fracture. Various concrete prisms are investigated with a particle density $P_k = 35\%$ with regular lattice and with the homogenous case of a one-phase cement matrix ($P_k = 0\%$) with regular and random lattices. The specimen sizes were varied in two- and three dimensions.

The results from the simulations show that a size effect exists: a growing specimen height (or volume) leads to a reduction of the nominal strength σ . The $\sigma - V$ relationship can be described by means of a single power-law, regardless of the three scaling types used. This stands in contrast to the $\sigma - H$ relationship, where for each case study (I to III) separate power-laws are required.

This lead to the idea to investigate and to compare the strength of specimens with varying prism sizes while maintaining their volumes. The results given so far show that the calculated strengths have similar values, regardless of the five shapes used, as long as the volumes were kept constant. On a $\log \sigma - \log V$ plot, the results from the shape analyses fall on the same lines as the points from the first three case studies (I-III), see [Figure 9](#). The present study is limited to the homogeneous case of a cement matrix ($P_k = 0\%$) and has to be extended for realistic particle densities for concrete.

ACKNOWLEDGMENTS

The authors thank the CSCS (Centro Svizzero di Calcolo Scientifico) in Manno (TI), Switzerland, for giving the opportunity to perform the numerical simulations on the CRAY XT3.

The authors also thank Mrs. Chiara Corticelli for her support in generating the particle structure.

REFERENCES

- Herrmann, H., A. Hansen, and S. Roux (1989). Fracture of disordered elastic lattices in two dimensions. *Physical Review B* 39(1), 637–648.
- Hrennikoff, A. (1941). Solutions of problems of elasticity by the framework method. *Journal of Applied Mechanics* 12, 169–175.
- Lilliu, G. and J.G.M. van Mier (2003). 3D lattice type fracture model for concrete. *Engineering Fracture Mechanics* 70, 927–941.
- Lingen, F.J. (2000). *Design of an object-oriented finite element package for parallel computers*. Ph. D. thesis, TU Delft.
- Man, H.-K. and J.G.M. van Mier (2006). Simulation of 2D and 3D Fracture Scaling using 3D Lattice Model. *Engineering Fracture Mechanics* (submitted).
- Man, H.-K. and J.G.M. van Mier (2007). Influence of Particle Density on 3D Size Effects in Concrete. (submitted).
- Schlangen, E. (1993). *Experimental and Numerical Analysis of Fracture Processes in Concrete*. Ph. D. thesis, TU Delft.
- Schlangen, E. and J.G.M. van Mier (1992). Experimental and numerical analysis of micromechanism of fracture of cement based composites. *Cement Concrete Composites* 14, 105–118.
- Van Mier, J.G.M. (2004). Reality Behind Fictitious Cracks? In V. Li, C. Leung, K. Willam, and S. Billington (Eds.), *5th International Conference on 'Fracture of Concrete and Concrete Structures' (FraMCoS-V)*, pp. 11–30.
- Van Vliet, M.R.A. (2000). *Size Effect in Tensile Fracture of Concrete and Rock*. Ph. D. thesis, TU Delft.